The Use of Newly Assimilated Photosynthates by Soil Autotrophic and Heterotrophic Respiration on a Diurnal Scale

Moeka Ono¹, Bhaskar Mitra², Benju Baniya¹, Dohee Kim¹, Asko Noormets¹

¹Department of Ecology and Conservation Biology, Texas A&M University, College Station, TX, United States

²Information and Computational Science Department, The James Hutton Institute, Aberdeen, UK

Correspondence to: Moeka Ono (mono@tamu.edu) and Asko Noormets (noormets@tamu.edu)

Abstract

The regulatory role of plant carbohydrate status and root exudation on soil CO₂ efflux has been demonstrated, yet the underlying mechanisms, particularly through root respiration, remain largely theoretical. In this study, we analyzed the cospectral variation of soil autotrophic (Ra) and heterotrophic (Rh) respiration components with key physiological and environmental factors, including gross primary productivity (GPP), photosynthetically active radiations (PAR), soil temperature (Ts) and volumetric water content (VWC), to evaluate their relative contributions in a subtropical mature shortleaf pine forest in the southern United States. The findings reveal a strong diurnal relationship between Rh and both GPP and PAR, in contrast to the weaker and more variable associations observed with Ra. This suggests that substrate availability was a key limitation of Rh on a diurnal basis, and that recently assimilated carbohydrates were directly discharged into the soil via root and mycorrhizal exudates. The consistent 2–4 hour time lag between Rh relative to GPP is consistent with the propagation rate of phloem pressure-concentration waves. While a diurnal peak in Rh-Ts covariance was also detected, the time lag of Rh in relation to Ts varied between positive and negative values, precluding this from being a causal relationship. Ra had a similarly strong cospectral peak with GPP as Rh, but with inconsistent lag, likely because of carbon availability from local starch reserves.

1 Introduction

20

In the global carbon (C) cycle, soil CO₂ efflux (SR) is a major terrestrial C flux, estimated at 89 Pg C year⁻¹ (range: 68–101 Pg C year⁻¹) (Hashimoto et al., 2023; Jian et al., 2021), approximately nine times greater than annual fossil fuel emissions (Friedlingstein et al., 2022), and serves as the primary pathway for returning plant-assimilated CO₂ to the atmosphere. SR arises from the combined respiration of plant roots, bacteria, and rhizosphere microbes, with carbohydrates (CHO) translocated from photosynthetic tissues playing an essential role in sustaining this flux (Kuzyakov & Gavrichkova, 2010). Autotrophic respiration (Ra), including root and mycorrhizal respiration, is, in principle, directly fueled by CHO translocated belowground (Fenn et al., 2010; Heinemeyer et al., 2012). Heterotrophic respiration (Rh), particularly rhizosphere microbes, is also linked to photosynthesis through above- and belowground detritus production and rhizodeposition, including exudates that provide

labile C inputs, which are estimated to be around 1–3% of a forest's net primary productivity (NPP) (Phillips et al., 2008; Yin et al., 2014). The recent demonstration of tight coupling between SR and GPP (Han et al., 2014; Heinemeyer et al., 2012; Mitra et al., 2019) suggests that the pattern is driven by root respiration as mediated by the diurnal fluctuation in plant CHO status. With Rh being further removed from the CHO source, the primary C inputs (i.e., detritus) varying on a seasonal scale, and reports of lower temperature sensitivity of Rh than Ra (Reichstein et al., 2005), it has often been viewed as a more invariable, baseline process. However, direct evidence for such differentiation remains limited. Furthermore, most SR upscaling models do not explicitly consider substrate availability, and confound seasonal and diurnal temperature (Davidson et al., 2006) and moisture (Davidson et al., 1998; Li et al., 2008) sensitivities (Martin et al., 2012).

The allocation of CHO belowground depends on the relative strength of different C sinks in plants, which, in turn, may be restricted by water and nutrient availability (Jiang et al., 2020; Körner, 2015; Sevanto & Dickman, 2015), physiological state, and hormones (Herms & Mattson, 1992), all of which vary seasonally and respond to stresses (Gessler & Zweifel, 2024). As summarized in the "surplus carbon hypothesis" (Prescott et al., 2020), overwhelming evidence supports the view of a passive, sink-strength-driven nature of C allocation, with implications for C cycling and responses to stressors, such as drought and nutrient limitations (Prescott, 2022; Prescott et al., 2020). Surplus CHO that are not used in aboveground growth and maintenance can be stored (as starch or lipids), converted to secondary compounds, or translocated from leaves to belowground compartments, where they can support root and mycorrhizal growth, or be exuded into the soil. The sink-strength-driven allocation model implies that this process helps regulate CHO concentrations in cells, preventing them from reaching levels that could become toxic to cellular processes (McClain & Sharkey, 2019). However, quantifying the interactions between CHO translocation and CO₂ release remains challenging due to the complexity of these mechanisms.

50

The timescale and level of coupling between photosynthetic C uptake and soil processes are confounded by plant physiological processes that can introduce variable lags to C transport from leaves to different plant organs, including the sink strength of different tissues, mycorrhizal associations, and the rate of phloem transport (Canarini et al., 2019; Sevanto & Dickman, 2015), as well as by methodological effects. Much of our current understanding of C allocation originates from stable isotope labeling studies, in which the progressive detection of isotopically labeled C in different tissues has been tracked (e.g., Epron et al., 2012; Gessler et al., 2007; Högberg et al., 2008; Kodama et al., 2008; Wingate et al., 2010). These studies show that the newly assimilated C can be translocated from leaves of a tree to the roots on the order of a day or two (Mencuccini & Hölttä, 2010; Moyano et al., 2008). Yet, our earlier analysis (Mitra et al., 2019), as well as those of others (Vargas et al., 2011; Vargas et al., 2010), detected a diurnal cospectral peak between SR and CHO availability, indicated by photosynthetically active radiation (PAR) or net ecosystem exchange (NEE), on the order of hours, which is attributable to plant carbohydrate status responding via pressure-concentration waves (Thompson & Holbrook, 2004). Finally, additional coupling with potentially variable lags may be introduced by soil heterotrophs, where the C subsidy by plant exudates may serve as a free substrate for their metabolism. For example, Yang et al. (2022) demonstrated a strong correlation between microbial respiration and PAR in a

subtropical forest with a lag of a few hours, underscoring the tight coupling between recent photosynthetic inputs and soil microbial activity. Such inputs can also trigger priming of the decomposition of old recalcitrant soil C, by providing energy (and possibly substrate) for the production of more resource-intensive enzymes (Jilling et al., 2025; Meier et al., 2017).

Here, we report the coherence of Rh and Ra with key physiological and environmental drivers, gross primary productivity (GPP), PAR, soil temperature, and soil moisture, with the focus on the diurnal timescale. We hypothesized that GPP is the primary driver of diurnal variations in Ra, while soil temperature and moisture predominantly regulate Rh, with influences spanning diel and synoptic scales. Quantitative understanding of the coupling between respiration components and GPP may help address key remaining uncertainties in ecosystem carbon cycle models (Lawrence et al., 2019; O'Sullivan et al., 2022).

2 Materials and Methods

2.1 Study Site

The study was conducted at the US-CRK Ameriflux site, a fire-managed mature shortleaf pine forest in Davy Crockett National Forest, TX (31.4629 N, 95.3415 W), in a humid subtropical climate region. The average annual precipitation and annual temperature are 1148 mm and 19.1 °C, respectively. The soil type at this site is classified as moderately well-drained Latex loam. The majority of fine root biomass (84%) was concentrated in the top 30 cm of soil at the site (Fig. S1). The site is maintained through biannual prescribed burning, and the recent burning took place in the winters of 2022 and 2024, although the fire's effect on the measurement area was minimal. The overstory vegetation within the study site is primarily dominated by shortleaf pine (*Pinus echinata*), with lesser amounts of loblolly pine (*Pinus taeda*), American sweetgum (*Liquidambar styraciflua*), and post oak (*Quercus stellata*). The stand average tree diameter at breast height was 33.1 ± 1.60 cm, the mean tree height was 25.8 ± 1.47 m, and the estimated aboveground biomass was 15.4 ± 0.06 kg m⁻² year⁻¹ in 2021.

2.2 Continuous Soil Respiration Measurements

Continuous soil respiration measurements were conducted hourly from May 2022 through October 2024 using an infrared gas analyzer (LI-8100A, LI-COR Biosciences, Lincoln, NE, USA) equipped with three long-term chambers (LI-8100-101 and LI-8100-104, LI-COR Biosciences). Chambers were installed over shallow (5cm tall) or deep (35 cm) polyvinyl chloride (PVC) collars. Shallow collars were inserted 2–3 cm into the soil and used to quantify total soil CO₂ efflux (SR), while deep collars were inserted approximately 25 cm into the soil to sever roots and capture root-excluded heterotrophic soil CO₂ efflux (Rh). Collars were initially installed in April 2022 and relocated in April 2023, October 2023, and June 2024 to maintain effective root severance in deep collars (Ono et al., 2025). Only periods during which the CO₂ efflux ratio between paired deep and shallow collars had stabilized, validated against manual survey measurements across five surrounding study plots, were included in the analysis (McElligott et al., 2016). The paired shallow and deep collars were placed at similar microsites, at a similar distance (approx. 2–3 m) from the nearest tree, and ensuring that initial soil CO₂ efflux rates would not differ more

than 10%. Aboveground vegetation within collars was clipped monthly to maintain bare-soil conditions. The spatial representativeness of the single automated system was further supported by comparison with 25 pairs of similar paired collars at five study plots and measured for three years. Autotrophic respiration (Ra) was estimated by the difference between SR and Rh during periods when Rh was deemed stable. The stable usable estimates of partitioned Rh (and Ra) occurred typically between 3 and 6 months after deep collar insertion (Ono et al., 2025). Soil CO₂ efflux declined during the first 2–3 months of the deep collar insertion as root internal carbohydrate reserves were being depleted. After about 6–8 months, the CO₂ efflux in the deep collars began to increase as the dead roots became additional substrate for heterotrophs.

Six measurement periods (hereafter referred to as campaigns), each spanning approximately 3–4 weeks, were identified from the continuous dataset. They were determined by the simultaneous availability of high-quality gross primary productivity (GPP), SR, Rh, photosynthetically active radiation (PAR), soil temperature (Ts), and volumetric water content (VWC) data. The six campaigns included two early growing seasons (C1, C4), one late growing season (C5), and three dormant or cool seasons (C2, C3, C6) (Table 1, Fig.1). The categorization into seasons was based on physiological state, including canopy leaf area index (LAI), GPP, and SR values, as well as soil temperature and moisture conditions. Importantly, the vegetation was active throughout the year, and the "dormant" periods were characterized merely by lower GPP (and LAI and SR), not their cessation.

2.3 Micrometeorological Parameters

105

110

115

Photosynthetically active radiation (PAR) was measured half-hourly above the canopy at a height of 43 m (PQS1, Kipp & Zonen, Delft, Netherlands). Soil temperature (Ts) and volumetric water content (VWC) were recorded half-hourly at 5 and 20 cm depth with CS108 and CS650 probes, respectively (both by Campbell Scientific, Logan, UT, USA). Half-hourly gross primary productivity (GPP) was estimated by partitioning the net ecosystem exchange of CO₂ into GPP and ecosystem respiration using the nighttime partitioning approach in the "Reddyproc" package in R (Wutzler et al., 2022). Specific details of eddy covariance data processing are reported by Baniya et al. (2025). All parameters were aggregated to hourly values for analysis, to match the frequency of continuous SR data.

The leaf area index (LAI) at the site was extracted from the Moderate Resolution Imaging Spectroradiometer (MODIS; MCD15A3H Version 6.1), which provides 4-day composite estimates for a 500-meter pixel centered on the study site (Myneni et al., 2021). Peak LAI estimates were verified against on-site measurements with a LAI-2000 Plant Canopy Analyzer (LI-COR Biosciences) in August 2023. Both estimates matched within 0.2 m² m⁻² (data not shown).

2.4 Data Analysis

All data analyses were performed in R (version 4.3.3) (R Core Team, 2024) and implemented in RStudio (version 2023.12.1) (Posit team, 2024).

2.4.1 Quality Control of Soil Respiration Components

Occasional abnormal spikes in the soil respiration data time series were observed, often due to gas analyzer failure or interference from small animals. To ensure the data quality for subsequent analyses, these anomalies were removed using the following quality control criteria: (1) poor model fit for flux calculation ($R^2 < 0.975$), (2) high coefficient of variation (CV > 1.9), (3) negative flux values, and (4) insufficient flow rate.

2.4.2 Spectral Analysis

130

135

140

145

150

155

We analyzed the wavelet spectra of soil respiration components (Ra and Rh, or their residuals, r_{Ra} and r_{Rh}; Section 2.4.3) and their cospectra with environmental and physiological drivers (GPP, PAR, Ts, and VWC) in the time-frequency domain. The most straightforward analysis quantifies the covariance of each flux with the four drivers. However, if we assume, like some earlier analyses have done (Liu et al., 2006; Vargas et al., 2011), that the primary driver of respiration fluxes is temperature, the contribution of additional drivers can be evaluated considering their covariance with the residuals of the temperature response model. Therefore, the cospectral analyses of the residuals were included to verify the consistency of the conclusions. And given that diurnal and synoptic temperature responses of respiration can differ drastically, the residuals were calculated for each (section 2.4.3). The residual analyses were consistent with and confirmed the conclusions based on the cospectral analyses with fluxes Ra and Rh (Figs. S3–S13). Similarly, the spectral analyses were completed for data where campaigns C3–C4 and C5–C6 were not separated into active and dormant periods. The results showed similar cospectral peaks and similar patterns in lag times between respiration components (Ra and Rh) with potential drivers (GPP, PAR, Ts, and VWC). Only the standard deviations of time lags were larger with the longer averaging periods. Therefore, we chose to subdivide the data into 6 instead of 4 campaigns, as the differences in flux magnitudes may also signify changes in underlying physiology.

Briefly, the continuous wavelet transformation was performed using the Morlet wavelet as the basis function (Grinsted et al., 2004). We applied wavelet transformation (WT) for a single time series (e.g., Rh, Ra) and cross-wavelet transformation (XWT) for analyzing the relationship between two time series (e.g., Rh vs GPP), following the methodological framework described by Mitra et al. (2019). The time series data were normalized to zero mean and unit variance, and occasional gaps were filled using zero padding. To align with the temporal scales of interest, the analysis focused on frequencies corresponding to time intervals from 6 hours to 64 days. For the phase angle analysis between effects (i.e., Rh and Ra) and drivers, we focused on the diurnal frequency range (0.5 to 1.5 days). Phase differences within this range were averaged but included only when the spectral peak at the 1-day period was statistically significant (p < 0.1). Daily mean phase angles were then converted to time lags (in hours) using Lag (hours) = (mean phase angle \times 24) / (2 π). To prevent introducing artifacts, phase angle values during padded gaps were excluded. The statistical significance of WT and XWT analyses was evaluated within the cone of influence (COI) at a 5% significance level using Monte Carlo methods (100 simulations). The surrogate data for significant analysis was generated using white noise (the color of the noise has little impact on the results; Grinsted et al., 2004; Vargas et al., 2010).

The cospectral analysis was performed using the "analyze coherency" function in the "WaveletComp" package in R (Roesch & Schmidbauer, 2018).

2.4.3 Residual Analysis

We also analyzed the temperature- and GPP- (or PAR-) controlled components of Ra and Rh by first removing the temperature dependence by exploring the cospectra of the potential drivers with the residuals of the measured and modeled Ra and Rh (r_{Ra} and r_{Rh}) (Liu et al., 2006; Vargas et al., 2011). Ra and Rh were modeled using the Q₁₀ function (van't Hoff (1898) as cited in Lloyd and Taylor (1994)):

$$R_{model} = R_{20} \times Q_{10}^{\frac{T_{S5}-20}{10}}, \tag{1}$$

where R_{model} is the modeled respiration component at soil temperature (T_{s5}) at 5 cm depth, R_{20} is the reference respiration at 20 °C, and Q_{10} is the temperature sensitivity coefficient. Spectral analysis of T_{s5} revealed consistent diurnal and weekly peaks across campaigns (Figs. 3M–R; see section 3.2). Therefore, we estimated coefficients (R_{20} and Q_{10}) at two window lengths to isolate temperature responses at these timescales: a daily window to track diurnal variability and a 7-day rolling window to capture slower variability. The corresponding residuals were denoted as r_{Rh_day} (or r_{Ra_day}) and r_{Rh_week} (or r_{Ra_week}), respectively. Coefficients were estimated by minimizing the residual sum of squares through nonlinear least-squares analysis using the "nls table" function in the "forestmangr" package in R (Braga et al., 2023).

3 Results

165

170

180

175 3.1 Soil Respiration and Environmental Conditions

Across the six measurement campaigns, SR ranged from 1.69 ± 0.81 to 5.05 ± 1.03 µmol CO₂ m⁻² s⁻¹, Rh from 1.05 ± 0.40 to 2.46 ± 0.32 µmol CO₂ m⁻² s⁻¹ and Ra 0.43 ± 0.38 to 2.70 ± 0.84 µmol CO₂ m⁻² s⁻¹ (Table 1, Figs. 1A–D). Maximum effluxes for SR and Ra were recorded in C1, which corresponded to the highest GPP and LAI (Table 1). On the other hand, lower SR, Rh, and Ra were observed during dormant-season campaigns (C2, C3, and C6). Rh consistently accounted for the majority of SR, contributing 59–86% across campaigns, except for C1, when its contribution was 47%. The Rh:SR ratio was greater during the dormant season (0.79 \pm 0.08, n = 3) than the growing season (0.63 \pm 0.19, n = 3), but the difference was not statistically significant (one-way ANOVA, p = 0.26). VWC during C3 and C4 was among the highest, driven by sustained rainfall in early 2024, whereas C5 and C6 experienced the lowest values due to drought conditions.

Table 1. Mean site conditions and fluxes during the six measurement campaigns (Mean ± standard deviation). Soil temperature (Ts5; °C) and volumetric water content (VWC5; %) at a depth of 5 cm, total soil respiration (SR; μmol m⁻² s⁻¹), heterotrophic respiration (Rh; μmol m⁻² s⁻¹), autotrophic respiration (Ra; μmol m⁻² s⁻¹), the ratio of Rh to SR (Rh:SR; unitless), daylight-period gross primary productivity (GPP; μmol CO₂ m⁻² s⁻¹), and leaf area index derived from MODIS (LAI; m² m⁻²). Campaigns conducted during active growing seasons are marked with an asterisk (*).

Campaign	Date	Ts ₅	VWC ₅	SR	Rh	Ra	Rh:SR	GPP	LAI
1*	2022-05-22 ~	24.1 ± 2.31	24.2 ± 1.78	5.05 ± 1.04	2.35 ± 0.45	2.70 ± 0.84	0.47 ± 0.08	14.3 ± 2.94	4.18 ± 0.79
	2022-06-09								
2	2023-03-15 ~	16.4 ± 2.57	23.4 ± 2.95	1.69 ± 0.81	1.05 ± 0.40	0.51 ± 0.43	0.71 ± 0.15	9.05 ± 2.53	1.68 ± 0.15
	2023-04-05								
3	2024-03-03 ~	16.6 ± 2.05	42.6 ± 0.66	1.79 ± 0.63	1.38 ± 0.39	0.44 ± 0.38	0.79 ± 0.16	8.31 ± 2.01	1.17 ± 0.40
	2024-03-31								
4*	2024-04-01 ~	19.2 ± 1.93	43.0 ± 0.52	2.15 ± 0.68	1.88 ± 0.42	0.43 ± 0.40	0.84 ± 0.18	11.6 ± 2.29	1.77 ± 0.90
	2024-04-27								
5*	2024-09-03 ~	24.7 ± 2.17	10.4 ± 2.14	4.20 ± 0.54	2.47 ± 0.32	1.73 ± 0.42	0.59 ± 0.07	11.1 ± 1.76	2.11 ± 0.41
	2024-09-30								
6	2024-10-01 ~	21.8 ± 2.62	4.11 ± 0.90	2.10 ± 0.50	1.78 ± 0.32	0.32 ± 0.31	0.86 ± 0.11	8.21 ± 1.85	1.75 ± 0.29
	2024-10-31								

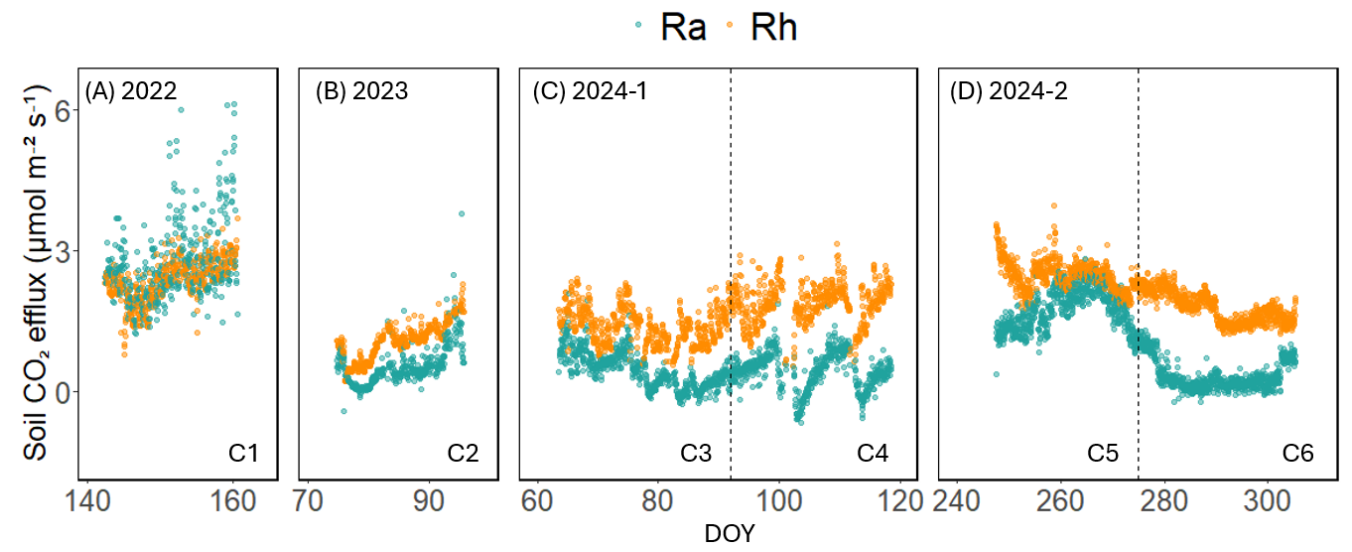


Figure 1. Hourly time series of soil autotrophic respiration (Ra, green) and heterotrophic respiration (Rh, orange) in μmol m⁻² s⁻¹ across six measurement campaigns (C1–C6) at the US-CRK between 2022 and 2024 (A–D).

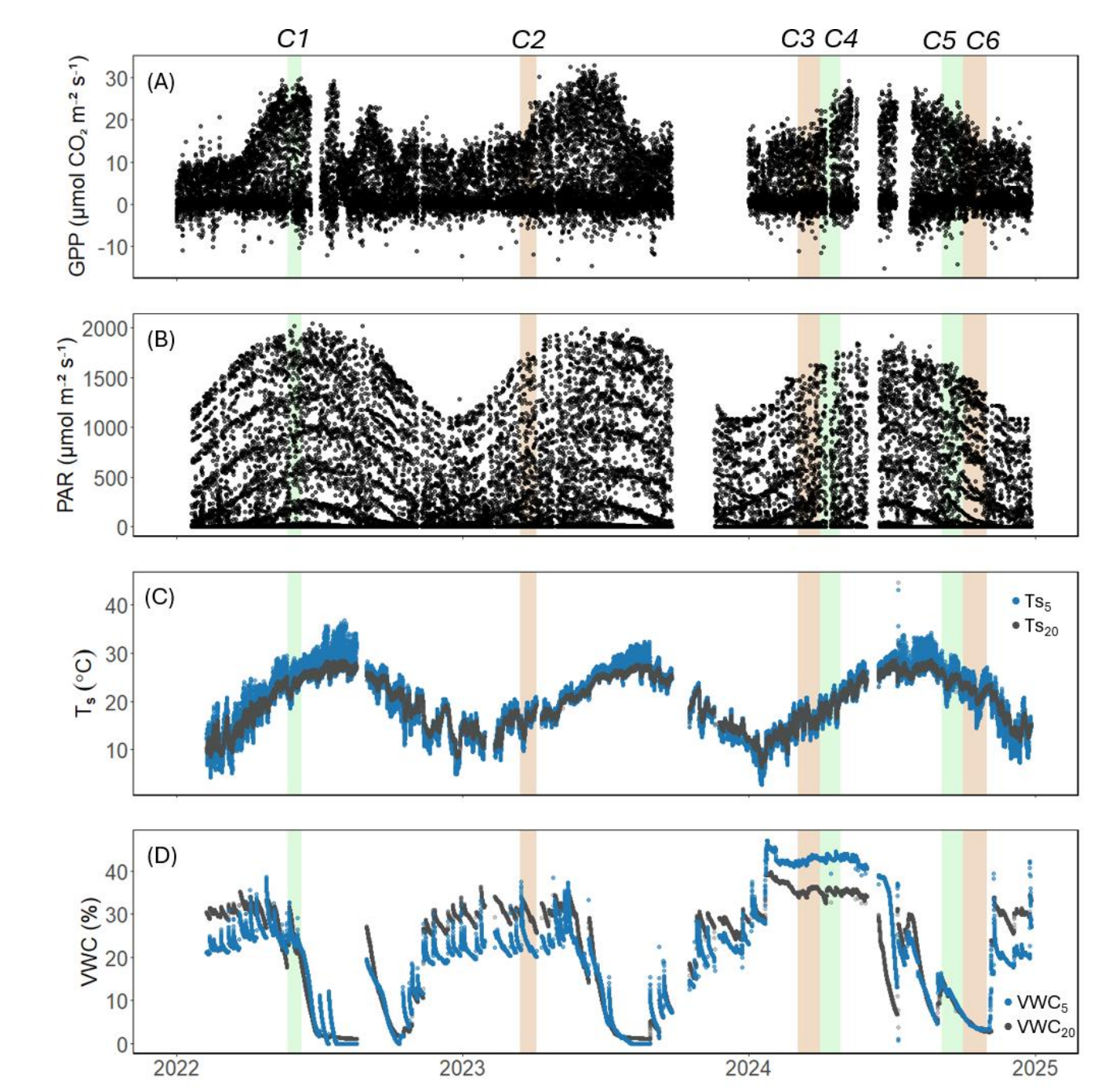


Figure 2. Hourly time series of (A) gross primary productivity (GPP; μmol CO₂ m⁻² s⁻¹), (B) photosynthetically active radiation (PAR; μmol m⁻² s⁻¹), (C) soil temperature (Ts₅ and Ts₂₀; °C), and (D) volumetric water content (VWC₅ and VWC₂₀; %) at 5 and 20 cm depth at the US-CRK site from 2022 to 2024. Shaded regions denote the six soil respiration measurement campaigns (C1–C6); green indicates active growing season campaigns, while brown indicates dormant season campaigns.

3.2 Spectral and Cospectral Characteristics

GPP and PAR consistently exhibited significant diurnal and subdiurnal spectral peaks across all six campaigns (Figs. 3A–L).

In contrast, Ts₅ displayed both significant diurnal and synoptic peaks, with the latter ranging from weekly to monthly timescales, while VWC₅ varied mostly at the synoptic scale (Figs. 3M–X). Rh showed significant diurnal spectral peaks in all campaigns, with more pronounced and distinct peaks during the growing season (C1, C4, and C5) and C3 (Figs. 4A–F). Synoptic peaks in Rh were also detected. Spectral analysis of Ra showed strong, significant diurnal peaks in C1 and weak but still significant diurnal peaks in C2, C3, and C5, along with detectable synoptic peaks (Figs. 5A–F).

205

210

Cospectral analysis showed that Rh exhibited significant diurnal peaks with GPP and PAR across all campaigns, with stronger diurnal peaks during the growing seasons (C1, C4, and C5) and in C3 (Figs. 4G–R, 6A–L). Ra also exhibited significant diurnal peaks with GPP and both subdiurnal and diurnal peaks with PAR, particularly during C1 and C5 (Figs. 5G–R, 7A–L). Although Ra-GPP cospectral power was slightly greater than that for Rh-GPP in C1 and C2, in C3–C6, Rh-GPP cospectral power exceeded that of Ra-GPP by a factor of 1.2 to 2.6-fold (p = 0.047; one-way ANOVA).

Cospectral analysis with Ts₅ demonstrated both significant diurnal and synoptic peaks for both Rh and Ra across campaigns (Figs. 4S–X, 5S–X). Notably, in C2, C3, and C4, cospectral peaks at weekly timescales were stronger than those at the diurnal timescale. While peaks extending beyond monthly timescales were observed for both Rh and Ra with Ts₅, they fell outside the cone of significance and were excluded from further interpretation. Rh and Ra also exhibited cospectral peaks with VWC₅ at synoptic scales (weekly to monthly). Significant diurnal peaks were detected only during C1, C3, and C4, but these were generally weaker and less consistent than those observed with GPP, PAR, and Ts₅ (Figs. 4Y–A4, 5Y–A4). Overall, their cospectral peaks at weekly scales were stronger than diurnal-scale peaks. The cospectral analysis with Ts₂₀ and VWC₂₀ also showed a similar pattern with Ts₅ and VWC₅, though the magnitude of the diurnal peaks was generally smaller (Fig. S2).

220

225

Cospectral analysis of model residuals (r_{Rh_day} and r_{Ra_day} , as well as r_{Rh_week} and r_{Ra_week}) with GPP and PAR showed overall patterns consistent with those of Rh and Ra. Diurnal peaks of r_{Rh_day} and r_{Rh_week} with GPP and PAR were consistently pronounced and significant across campaigns (Figs. S3 G–R, S7 G–R). Both r_{Ra_day} and r_{Ra_week} also exhibited consistently significant diurnal peaks with GPP and PAR (Figs. S4 G–R, S8 G–R), with particularly strong peaks of r_{Ra_day} observed during C5 and C6 (Figs. S4 K, L). The Q_{10} values for model residuals showed large variability across campaigns and between Rh and Ra, with particularly high and uncertain estimates for Ra during campaigns 3 and 4 (no data shown).

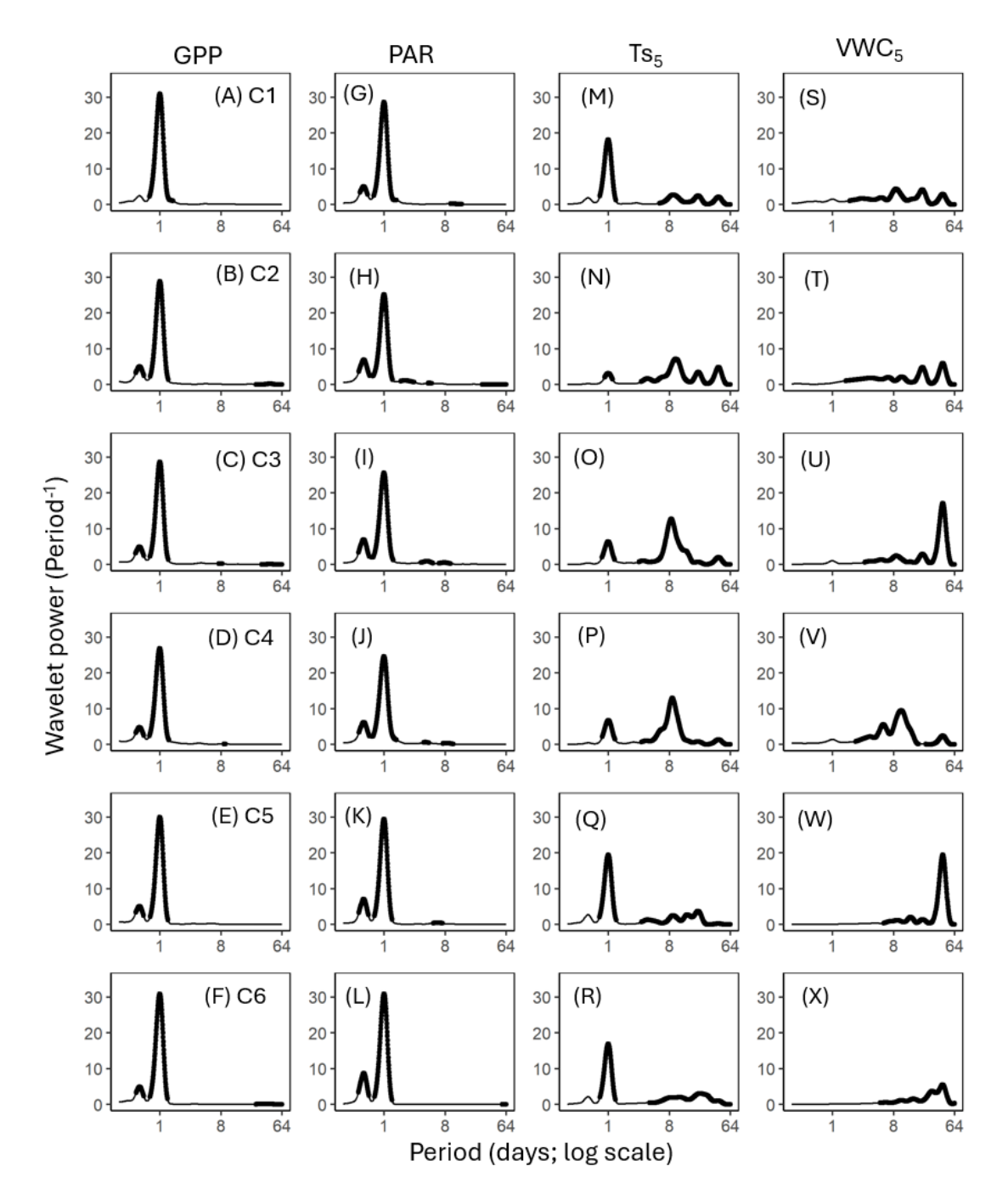


Figure 3. Average wavelet power in the frequency domain (Period; time intervals from 6 hours to 64 days) generated from the wavelet transformation of gross primary productivity (GPP; A–F), photosynthetically active radiation (PAR; G–L), soil temperature (Ts5; M–R), and volumetric water content (VWC5; S–X) at 5-cm depth for six campaigns (C1–C6) at US-CRK. The bold contours indicate areas with significant coherence at the 5% level against white noise.

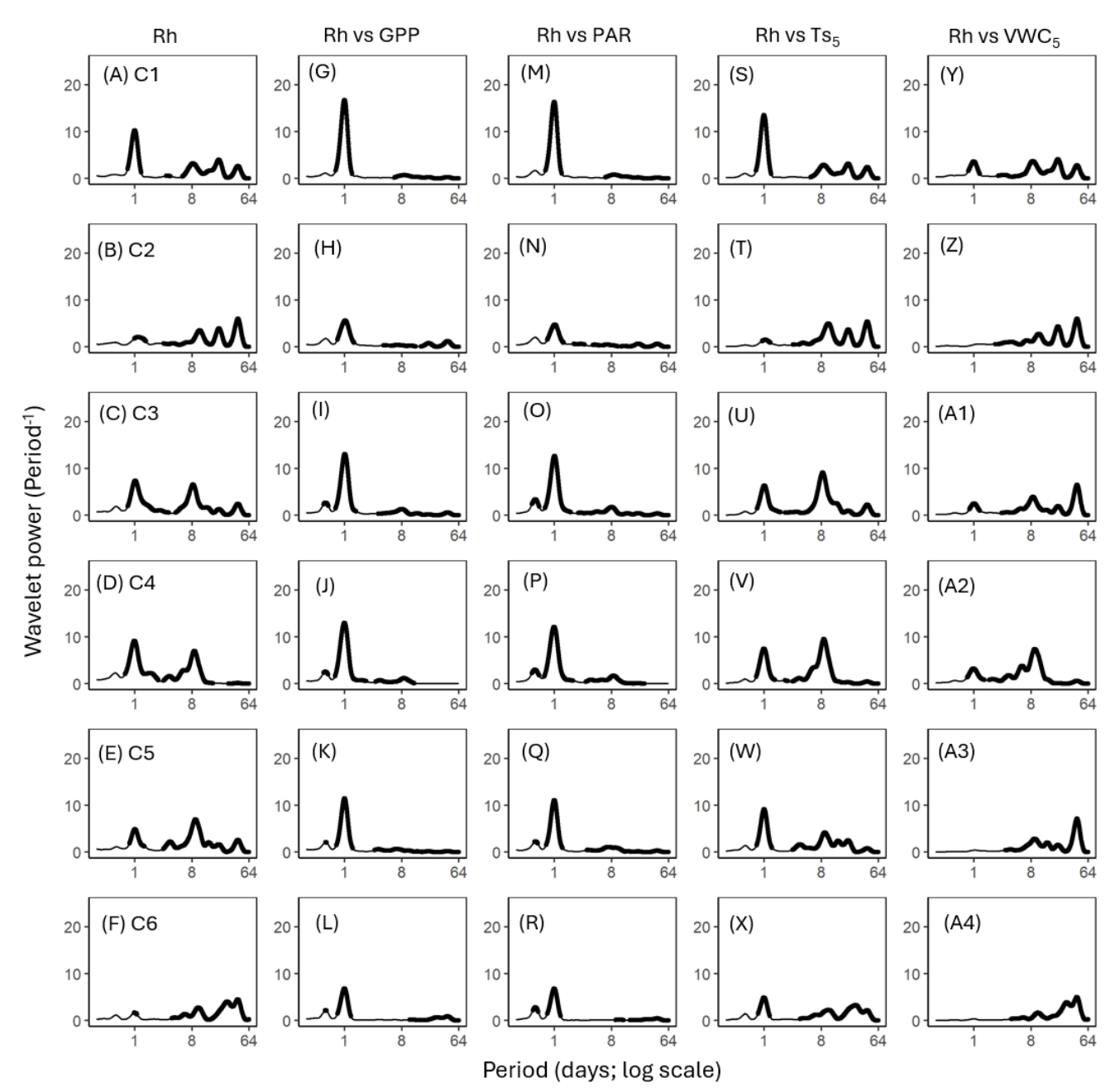


Figure 4. Average wavelet power in the frequency domain (Period; time intervals from 6 hours to 64 days) generated from the wavelet transformation of heterotrophic respiration (Rh; A–F) for six campaigns (C1–C6) at US-CRK. Average wavelet power in the frequency domain generated from the cross-wavelet transformation of heterotrophic respiration (Rh) against gross primary productivity (GPP; G–L), photosynthetically active radiation (PAR; M–R), soil temperature (Tss; S–X), and volumetric water content (VWCs; Y–A4) at 5-cm depth for six campaigns at the US-CRK site. The bold contours indicate areas with significant coherence at the 5% level against white noise.

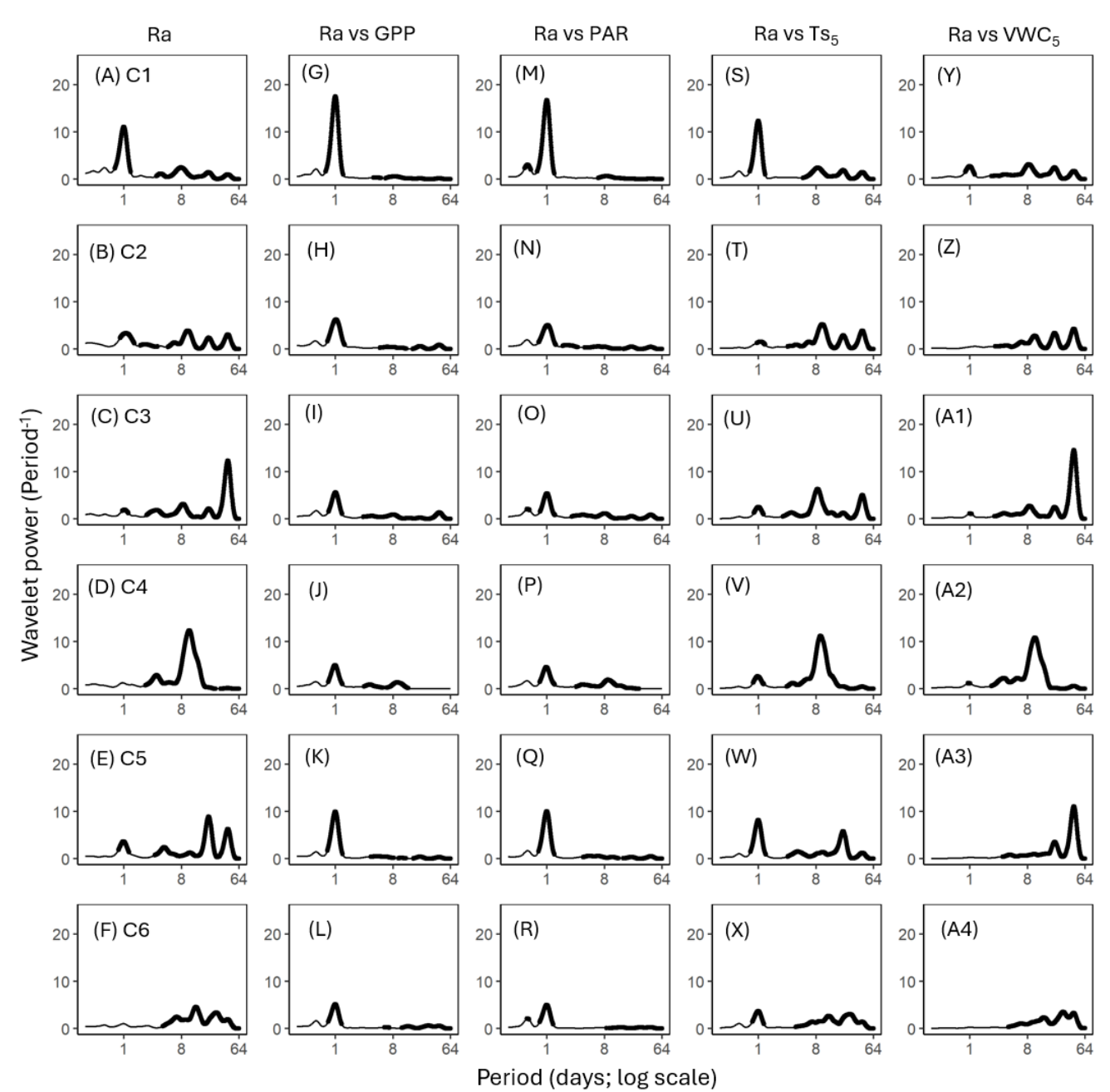


Figure 5. Average wavelet power in the frequency domain (Period; time intervals from 6 hours to 64 days) generated from the wavelet transformation of autotrophic respiration (Ra; A–F) for six campaigns (C1–C6) at US-CRK. Average wavelet power in the frequency domain generated from the cross-wavelet transformation of heterotrophic respiration (Rh) against gross primary productivity (GPP; G–L), photosynthetically active radiation (PAR; M–R), soil temperature (Tss; S–X), and volumetric water content (VWC5; Y–A4) at 5-cm depth for six campaigns at the US-CRK site. The bold contours indicate areas with significant coherence at the 5% level against white noise.

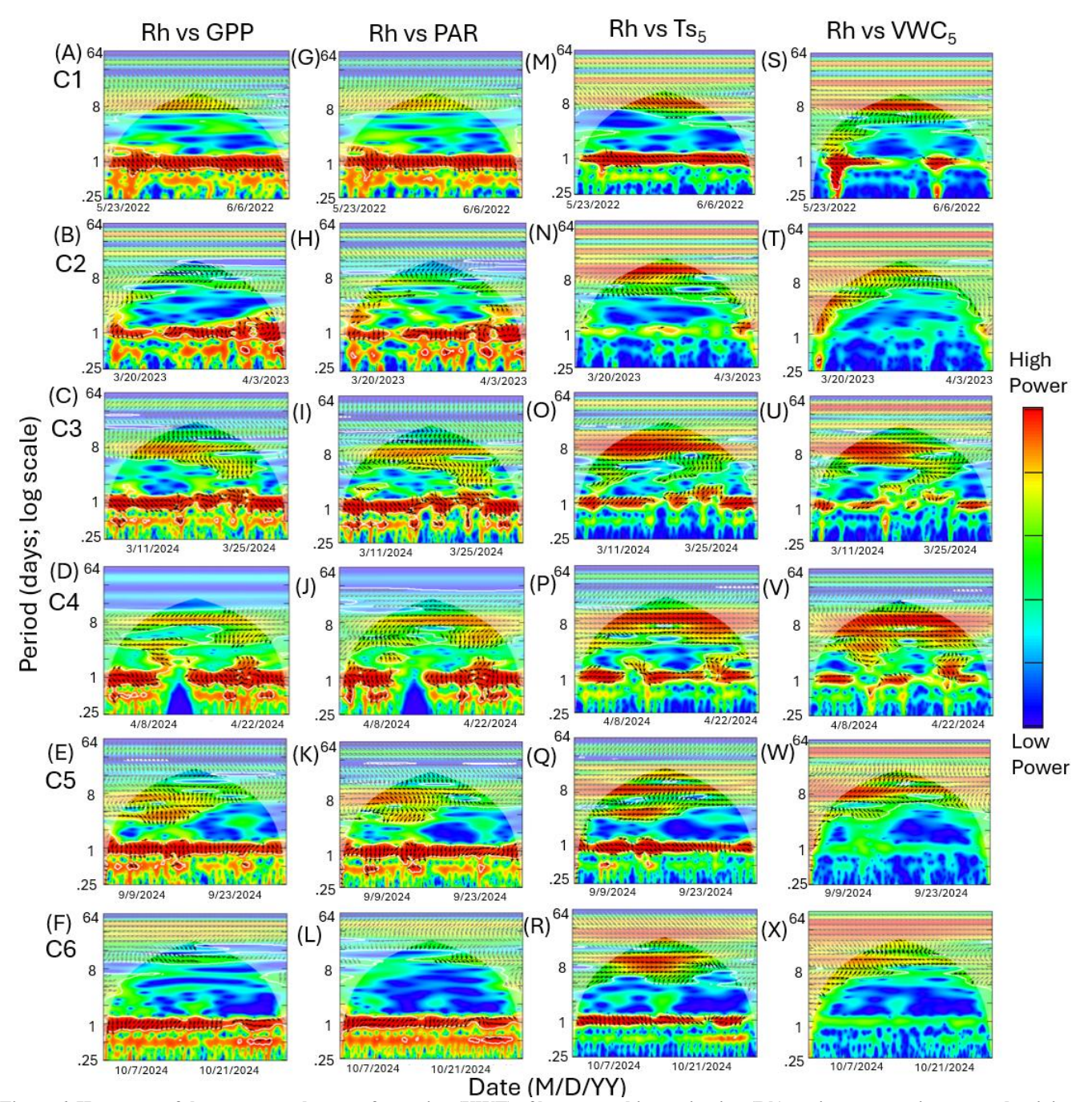


Figure 6. Heatmaps of the cross-wavelet transformation (XWT) of heterotrophic respiration (Rh) against gross primary productivity (GPP; A–F), photosynthetically active radiation (PAR; G–L), soil temperature (Ts₅; M–R), and volumetric water content (VWC₅; S–X) for six measurement campaigns (C1–C6) at US-CRK. Arrows pointing to the right and left represent positive and negative correlations, respectively, without lag. Arrows pointing up-left (positive correlation) and down-right (negative correlation) indicate the response component lags behind the driver, while arrows pointing up-right and down-left indicate that the driver lags behind the response component. The 5% significance level of the XWT analysis was generated within the cone of influence (COI) against white noise and identified by white contour lines. COI within the heat plot is identified with a light shade.

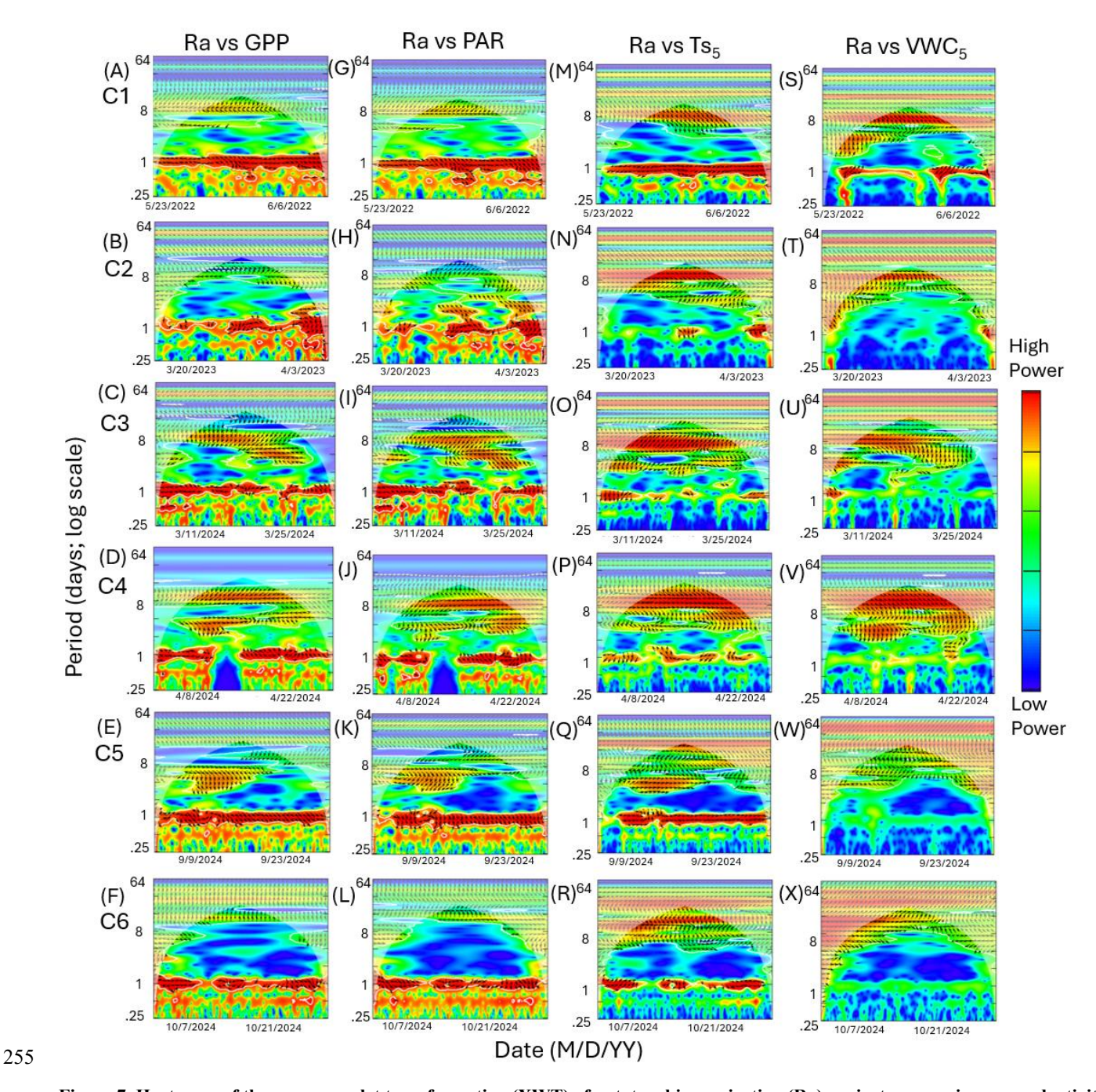


Figure 7. Heatmaps of the cross-wavelet transformation (XWT) of autotrophic respiration (Ra) against gross primary productivity (GPP; A–F), photosynthetically active radiation (PAR; G–L), soil temperature (Tss; M–R), and volumetric water content (VWC5; S–X) for six measurement campaigns (C1–C6) at US-CRK. Arrows pointing to the right and left represent positive and negative correlations, respectively, without lag. Arrows pointing up-left (positive correlation) and down-right (negative correlation) indicate the response component lags behind the driver, while arrows pointing up-right and down-left indicate that the driver lags behind the response component. The 5% significance level of the XWT analysis was generated within the cone of influence (COI) against white noise and identified by white contour lines. COI within the heat plot is identified with a light shade.

3.3 Phase Analysis

At the diurnal frequency range, the phase differences between Rh and both GPP and PAR revealed consistent lag patterns, with Rh lagging behind GPP by 1.9–4.2 hours and behind PAR by 2.5–4.3 hours across campaigns (Figs. 8A, B). In contrast, the phase relationships between Ra and GPP or PAR were more variable, with lag-lead times ranging from -1.7 to +4.2 hours for GPP and -3.1 to +5.7 hours for PAR, showing inconsistent patterns (Figs. 8D, E). Notably, during drought (C5 and C6), the lag time of Ra relative to GPP (C5: -1.7 hour; C6: -1.7 hour) was shorter than that of Rh (C5: -4.2 hour; C6: -3.3 hour). Phase angle analysis using model residuals showed similar results, where r_{Rh_day} lagged GPP by -3.5 ± 0.42 hours on average, except during C2, which exhibited a slight lead of +0.64 ± 2.8 hours, and r_{Rh_week} lagged GPP by -5.7 to -0.02 hours (Figs. S11A, S12A). In contrast, r_{Ra_day} and r_{Ra_week} exhibited greater variability, with lag-lead times ranging from -1.9 to 2.1 hours and from +0.20 to 3.9 hours, respectively (Figs. S11D, S12D). The phase angles between Ts and Rh or Ra also varied, ranging from -3.8 to +2.2 hours for Rh and -3.9 to +1.5 hours for Ra, indicating an inconsistent lag-lead relationship at the diurnal timescale (Figs. 8C, F). Ts₅ consistently lagged behind GPP and PAR by 3.5 ± 1.1 hours and 4.6 ± 1.3 hours, respectively, across all campaigns (Fig. S13).

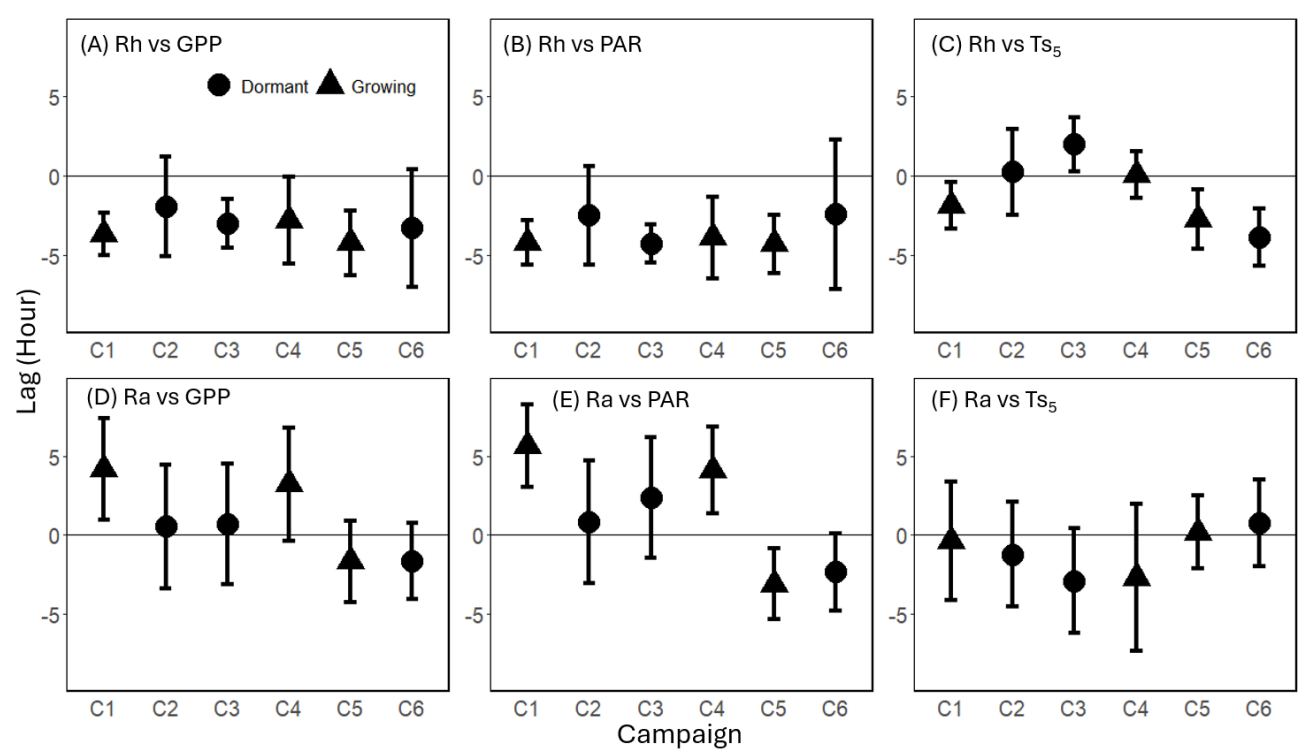


Figure 8. Mean time lag (± standard deviation) between heterotrophic respiration (Rh) in relation to (A) gross primary productivity (GPP), (B) photosynthetically active radiation (PAR), and (C) soil temperature (Tss), and between autotrophic respiration (Ra) with (D) GPP, (E) PAR, and (F) Tss at the diurnal frequency range (0.5 to 1.5 days) across six measurement campaigns (C1–C6). Phase differences were averaged over the diurnal frequency range and included only when the 1-day spectral peak was significant (p < 0.1). Round dots represent dormant season campaigns, while triangles represent growing season campaigns. Positive lag values indicate that respiration preceded the corresponding driver, while negative values indicate that respiration lagged behind the driver.

4 Discussion

290

295

4.1 Limitations and Uncertainties

This study lacks true replication, as measurements were conducted at a single system location. However, we report data from six measurement campaigns that span different seasons, vegetation physiological states, and soil water availability. The spatial representativeness of the continuous autochamber measurements of soil respiration measurements was validated against monthly manual survey measurements from 25 pairs of control and root exclusion collars located in five study plots over three years. A representativeness analysis (Baniya et al., 2025) indicated that the temporal dynamics of the SR, Ra, and Rh, as well as the heterotrophic fraction, were similar among all measurement locations, but the absolute magnitude of SR was slightly greater in plots with greater understory cover. Additionally, the observed Rh:SR ratio (59–86%) was comparable to the 36–84% recorded using the root exclusion method in our previous studies conducted in loblolly pine forest stands in East Texas that also experienced low-intensity prescribed burns with a return interval of 2–5 years (Ono et al., 2025), and consistent with other studies in loblolly pine chronosequences (McElligott et al., 2016) and among different ecosystems globally (Bond-Lamberty et al., 2018).

The partitioning of SR to Ra and Rh using the root exclusion method has its own limitations (Bond-Lamberty et al., 2011), and the partitioned fluxes are not fully independent. Ra and Rh are inherently interconnected through rhizodeposition, root exudation, and mycorrhizal associations (Kuzyakov & Gavrichkova, 2010), and CHO-priming further complicates their separation. In the current study, Rh was expected to be isolated from root activity and diurnal fluctuations in CHO supply. However, respiration from root-excluded soils (i.e., Rh) overall showed a stronger correlation with canopy photosynthetic activity (GPP and PAR) than did the flux attributed to Ra. This unexpected pattern suggests incomplete exclusion, potentially due to ingrowth of fine roots or mycorrhizal hyphae, or root activity below the collar. The influx of labile C compounds (presumably exudates) likely enhanced microbial activity within the collars, thereby coupling Rh with recent photosynthate supply.

Lastly, we acknowledge that this study did not directly quantify root exudation, microbial biomass, or enzyme activity, nor employ isotopic pulse-chase techniques. The inference about microbial activity is based solely on the cospectral analysis of fluxes described above, which, among the alternative approaches available, is considered the preferred tool for analyzing the coupling between plant and soil C dynamics (Mencuccini & Hölttä, 2010).

315 4.2 Multitemporal Relationship of Rh and Ra with GPP, PAR, Ts, and VWC

The initial hypothesis that Ra would be more sensitive than Rh to GPP on a diurnal scale was not supported by the results. Instead, Rh and r_{Rh} demonstrated strong diurnal correlations with both GPP and PAR, as evidenced by distinct diurnal

cospectral peaks (Figs. 4G-R, S2 G-R, S6 G-R) and heatmaps (Figs. 6A-L, S4 A-L, S8 A-L). The overall stronger diurnal cospectral relationship between Rh and GPP, compared to that of Ra and GPP, along with the consistent lag of Rh relative to GPP, rather than the more variable lag-lead patterns observed in Ra-GPP, suggests that the diurnal cycle of plant carbohydrate status was a key limiting factor for Rh, but was less pronounced for Ra. While Ra and r_{Ra} also exhibited diurnal cospectral peaks with GPP as well as the lag of Ra relative to GPP during C5 and C6 (Figs. 5K-L, S3 K-L), the time lag was reversed (Ra preceding GPP) during the first four campaigns. This suggests that tissue carbon status may have been buffered by starch reserves, as hydrolysis of stored starch can supply soluble sugars to meet the local energy and material demands (Zweifel et al., 2021). The strong response of Rh to plant C status during all measurement campaigns suggests an opportunistic microbial community. This is consistent with the findings of Yang et al. (2022), who reported a similar 2–6.5-hour lag of Rh relative to PAR across a year in a subtropical evergreen broadleaf forest, and contrasted it to a lack of such a pattern in an adjacent open canopy area. However, this contrasts with our initial hypothesis that the diurnal cospectral peaks would be mediated by fine root activity (Mitra et al., 2019). Many earlier studies that observed elevated soil CO₂ efflux closer to trees than away from them (e.g., Noormets et al., 2010; Savage et al., 2013; Tang et al., 2005) also assumed it must have been of autotrophic origin. In light of the results reported here, and those of Yang et al. (2022), Mitra et al. (2019), and Mitra et al. (2020), it should be acknowledged that while autotrophic respiration cannot be ruled out in those cases, there appears to be a rapid transfer of assimilated substrates from plants to soil microbes or simply exudation into the soil medium, and the processing of this newly assimilated carbon can be under microbial metabolic control.

335

340

320

325

330

The observed 2–4 hour lag of Rh relative to GPP at the diurnal scale is consistent with previously reported rates of pressure-concentration wave propagation in the phloem (Mencuccini & Hölttä, 2010) and the subsequent release into the rhizosphere (Kuzyakov & Gavrichkova, 2010). Although we did not directly measure exudate composition or microbial community responses, prior studies suggest that such rapid microbial utilization of new carbon inputs is facilitated by readily available substrates, such as soluble sugars and amino acids, that are tightly coupled with photosynthetic dynamics (Canarini et al., 2019). These labile compounds can activate microbes (Cheng et al., 2014; Kuzyakov & Blagodatskaya, 2015), and they can metabolize the compounds within hours (Kuzyakov & Gavrichkova, 2010). Therefore, we interpret it as a change in C availability (C status) in roots, with a likely pulse of exudation that triggered an increase in Rh within hours of enhanced photosynthetic activity, even though the mass flow of assimilates may occur over longer timescales (Liesche et al., 2015).

345

350

We did not observe pronounced seasonal differences in the diurnal cospectral peak strengths or lag-lead times for either Rh–GPP or Ra–GPP, in contrast to findings from other earlier studies (Heinemeyer et al., 2012; Yang et al., 2022). The reduced seasonal variation in our evergreen subtropical study site compared to that in deciduous forests is probably associated with the year-round photosynthetic capacity and metabolic activity. We also observed that allocation to non-structural carbohydrates remained positive even during the drought when growth ceased (C5–C6) (Baniya et al., 2025). This is consistent with earlier

reports that photosynthesis is less sensitive to drought than biomass production (Prescott et al., 2020), which may increase belowground carbon allocation and substrate availability to both Ra and Rh (further discussed in Section 4.3).

The phase angle differences between Ra and Rh with Ts showed mixed lag and lead relationships. Notably, in C1 and C5, the lag of Rh relative to Ts (1.9 and 2.7 hours, respectively; Fig. 8C) was shorter than its lag relative to GPP (3.7 and 4.2 hours, respectively; Fig. 8A), suggesting a potential functional connection between them (Mitra et al., 2019). However, the cospectral peak height was greater for Rh with GPP than with Ts (16.7 vs 13.5 period⁻¹ in C1, and 11.4 vs 9.1 period⁻¹ in C5; Figs. 4G, S, K, W), and the time lag between Rh and GPP (unlike that between Rh and Ts) was consistent across all campaigns, suggesting that carbohydrate transfer had a greater influence on Rh diurnal dynamics.

4.3 Implications and Future Considerations

355

365

370

375

380

The consistently strong cospectral peaks between Rh and GPP suggest that surplus photosynthates, not immediately allocated to plant growth, are exuded into the soil, where they appear to support the activity of the opportunistic microbial community. Ecosystem scale estimates of the magnitude of root exudation remain difficult to quantify, but at the current study site, the overall allocation to non-structural carbon compounds exceeded 100 g C m⁻² month⁻¹ in some months (Baniya et al., 2025). How much of it was retained in plants as storage compounds and how much was exuded into the soil, and whether these can be derived from the diurnal magnitudes of each flux (Fig. 1), remains to be determined, but there appears to be ample C available to support the exudation.

The current conclusion that the short-term (diurnal) variability in SR is primarily mediated by Rh and coupled to substrate availability from GPP appears to contrast most earlier interpretations (e.g., Heinemeyer et al., 2012; Savage et al., 2013; Tang et al., 2005), where the evidence appeared to support the link between GPP and Ra. However, in light of the present findings and those by Yang et al. (2022), it is possible that studies were the partitioning between Ra and Rh was based only on proximity to trees (Savage et al., 2013; Tang et al., 2005), without explicit root exclusion, may have measured CO₂ that was produced either by the roots and associated symbionts or by free-living microbes. If C exudation can fuel heterotrophs on a diurnal cycle and prime the decomposition of detritus, then separating these two fluxes conclusively becomes more difficult. Furthermore, if heterotrophic activity draws to a significant degree on newly assimilated photosynthates, it also calls into question the reliability of partitioning plant and microbial respiration based on Keeling plots (Pataki et al., 2003). This is illustrated by the recent study by Yang et al. (2022), who, on one hand, observed diurnal fluctuation only under a tree canopy and not in the open, but because root exclusion treatments were applied in both situations, were still able to attribute the signal to Rh instead of Ra.

Our findings lend support to the "surplus C theory" (Prescott, 2022; Prescott et al., 2020), whereby assimilation in excess of immediate plant needs may be stored or exuded. In the current study, campaigns C2–C6 coincided with low biomass

production, while C1 occurred during high growth (data not shown), yet during all of them, plants were estimated to have had excess non-structural carbohydrates (Baniya et al., 2025). It lends further support to the conclusion that carbon was exuded into the soil and consumed by heterotrophs. The current study adds to the body of evidence that increased photosynthesis does not always manifest in increased growth (Jiang et al., 2020), but can instead be exuded into the soil (Klein et al., 2016) or to mycorrhizal symbionts, where it may actually serve plant needs and support nutrient-acquiring enzymes (Hagenbo et al., 2019). The magnitude of exudation flux at different physiological states remains to be determined. It is notable that in the current study, this was observed during all six campaigns, spanning early, mid-, and late growing seasons.

The changing magnitudes and diurnal amplitudes of both Ra and Rh (Fig. 1) could be caused by both environmental and physiological constraints, and carbon allocation to different plant compartments likely responds to both. Future research will incorporate diel measurements of carbohydrate concentrations in tree and root tissues, isotopic partitioning of soil respiration, and multi-season campaigns to further evaluate the mechanisms underlying these observations.

Code and data availability. Meteorological data at the US-CRK can be downloaded from the Ameriflux database (Noormets, 2024). Continuous soil respiration data and all the code files for the analyses in this manuscript can be found on GitHub via https://github.com/moekaono/CRK_cont_SR.

400

405

Author contribution. MO: Writing – original draft, Visualization, Methodology, Investigation, Software, Formal analysis, Data curation, Conceptualization. BM: Writing – review & editing, Supervision, Methodology, Investigation, Software, Validation, Conceptualization. BB: Software, Investigation, Data curation, Writing – review & editing. DK: Data curation, Writing – review & editing. AN: Writing – review & editing, Supervision, Resources, Validation, Project administration, Methodology, Investigation, Funding acquisition, Conceptualization.

Competing interests. The authors declare that they have no conflict of interest.

Acknowledgments. Blaize Britton, Clement Sarpong, Malik Nkrumah, and Seth Massery assisted with soil sampling and soil CO₂ efflux measurements. MO was supported by the ITO Foundation and the McMillan-Ward Fellowship. DK and BB were supported by the Native Plant Society of Texas.

Financial support. This project was supported by USDA NIFA (award #: 2023-67019-40537), the Cynthia and George Mitchell Foundation, and the U.S. Department of Energy's Office of Science through the AmeriFlux Management Project (DE-AC02-05CH11231).

References

435

440

450

- Baniya, B., Kim, D., Nkrumah, M., Ono, M., Miao, G., & Noormets, A. (2025). Carbon Dynamics in a Shortleaf Pine Forest Amidst a Two-Year Drought. ESS Open Archive. https://doi.org/10.22541/essoar.175611350.04251050/v1
- 420 Bond-Lamberty, B., Bailey, V. L., Chen, M., Gough, C. M., & Vargas, R. (2018). Globally rising soil heterotrophic respiration over recent decades. *Nature*, 560(7716), 80-83. https://doi.org/10.1038/s41586-018-0358-x
 - Bond-Lamberty, B., Bronson, D., Bladyka, E., & Gower, S. T. (2011). A comparison of trenched plot techniques for partitioning soil respiration. *Soil Biology and Biochemistry*, 43(10), 2108-2114. https://doi.org/https://doi.org/10.1016/j.soilbio.2011.06.011
- Braga, S. R., Oliveira, M. L. R. d., & Gorgens, E. B. (2023). forestmangr: Forest Mensuration and Management. In (Version 0.9.6) https://CRAN.R-project.org/package=forestmangr
 - Canarini, A., Kaiser, C., Merchant, A., Richter, A., & Wanek, W. (2019). Root Exudation of Primary Metabolites: Mechanisms and Their Roles in Plant Responses to Environmental Stimuli [Review]. Frontiers in plant science, 10. https://doi.org/10.3389/fpls.2019.00157
- Cheng, W., Parton, W. J., Gonzalez-Meler, M. A., Phillips, R., Asao, S., McNickle, G. G., Brzostek, E., & Jastrow, J. D. (2014). Synthesis and modeling perspectives of rhizosphere priming. *New Phytologist*, 201(1), 31-44. https://doi.org/10.1111/nph.12440
 - Davidson, E. A., Belk, E., & Boone, R. D. (1998). Soil water content and temperature as independent or confounded factors controlling soil respiration in a temperate mixed hardwood forest. *Global Change Biology*, 4(2), 217-227. https://doi.org/10.1046/j.1365-2486.1998.00128.x
 - Davidson, E. A., Janssens, I. A., & Luo, Y. (2006). On the variability of respiration in terrestrial ecosystems: moving beyond Q₁₀. *Global Change Biology*, 12(2), 154-164. https://doi.org/10.1111/j.1365-2486.2005.01065.x
 - Epron, D., Bahn, M., Derrien, D., Lattanzi, F. A., Pumpanen, J., Gessler, A., Högberg, P., Maillard, P., Dannoura, M., Gérant, D., & Buchmann, N. (2012). Pulse-labelling trees to study carbon allocation dynamics: a review of methods, current knowledge and future prospects. *Tree Physiology*, 32(6), 776-798. https://doi.org/10.1093/treephys/tps057
 - Fenn, K. M., Malhi, Y., & Morecroft, M. D. (2010). Soil CO₂ efflux in a temperate deciduous forest: Environmental drivers and component contributions. *Soil Biology and Biochemistry*, 42(10), 1685-1693. https://doi.org/10.1016/j.soilbio.2010.05.028
- Friedlingstein, P., O'Sullivan, M., Jones, M. W., Andrew, R. M., Gregor, L., Hauck, J., Le Quéré, C., Luijkx, I. T., Olsen, A.,
 445

 Peters, G. P., Peters, W., Pongratz, J., Schwingshackl, C., Sitch, S., Canadell, J. G., Ciais, P., Jackson, R. B., Alin, S.
 R., Alkama, R.,...Zheng, B. (2022). Global Carbon Budget 2022. *Earth Syst. Sci. Data*, 14(11), 4811-4900.

 https://doi.org/10.5194/essd-14-4811-2022
 - Gessler, A., Keitel, C., Kodama, N., Weston, C., Winters, A. J., Keith, H., Grice, K., Leuning, R., & Farquhar, G. D. (2007). δ¹³C of organic matter transported from the leaves to the roots in *Eucalyptus delegatensis*: short-term variations and relation to respired CO₂. *Functional Plant Biology*, 34(8), 692-706. https://doi.org/10.1071/FP07064
 - Gessler, A., & Zweifel, R. (2024). Beyond source and sink control toward an integrated approach to understand the carbon balance in plants. *New Phytologist*, *n/a*(n/a). https://doi.org/10.1111/nph.19611
 - Grinsted, A., Moore, J. C., & Jevrejeva, S. (2004). Application of the cross wavelet transform and wavelet coherence to geophysical time series. *Nonlinear Processes in Geophysics*, 11(5/6), 561-566. https://doi.org/10.5194/npg-11-561-2004
 - Hagenbo, A., Hadden, D., Clemmensen, K. E., Grelle, A., Manzoni, S., Molder, M., Ekblad, A., & Fransson, P. (2019). Carbon use efficiency of mycorrhizal fungal mycelium increases during the growing season but decreases with forest age across a *Pinus sylvestris* chronosequence. *Journal of Ecology*, 107(6), 2808-2822. https://doi.org/10.1111/1365-2745.13209
- Han, G., Luo, Y., Li, D., Xia, J., Xing, Q., & Yu, J. (2014). Ecosystem photosynthesis regulates soil respiration on a diurnal scale with a short-term time lag in a coastal wetland. *Soil Biology and Biochemistry*, 68, 85-94. https://doi.org/10.1016/j.soilbio.2013.09.024
 - Hashimoto, S., Ito, A., & Nishina, K. (2023). Divergent data-driven estimates of global soil respiration. *Communications Earth & Environment*, 4(1), 460. https://doi.org/10.1038/s43247-023-01136-2

- 465 Heinemeyer, A., Wilkinson, M., Vargas, R., Subke, J. A., Casella, E., Morison, J. I. L., & Ineson, P. (2012). Exploring the "overflow tap" theory: linking forest soil CO₂ fluxes and individual mycorrhizosphere components to photosynthesis. Biogeosciences, 9(1), 79-95. https://doi.org/10.5194/bg-9-79-2012
 - Herms, D. A., & Mattson, W. J. (1992). The Dilemma of Plants: To Grow or Defend. *The Quarterly Review of Biology*, 67(3), 283-335. https://doi.org/10.1086/417659
- Högberg, P., Högberg, M. N., Göttlicher, S. G., Betson, N. R., Keel, S. G., Metcalfe, D. B., Campbell, C., Schindlbacher, A., Hurry, V., Lundmark, T., Linder, S., & Näsholm, T. (2008). High temporal resolution tracing of photosynthate carbon from the tree canopy to forest soil microorganisms. *New Phytologist*, 177(1), 220-228. https://doi.org/10.1111/j.1469-8137.2007.02238.x
- Jian, J., Vargas, R., Anderson-Teixeira, K. J., Stell, E., Herrmann, V., Horn, M., Kholod, N., Manzon, J., Marchesi, R., Paredes, D., & Bond-Lamberty, B. P. (2021). *A Global Database of Soil Respiration Data, Version 5.0* (ORNL Distributed Active Archive Center. https://doi.org/10.3334/ORNLDAAC/1827

490

- Jiang, M., Medlyn, B. E., Drake, J. E., Duursma, R. A., Anderson, I. C., Barton, C. V. M., Boer, M. M., Carrillo, Y., Castañeda-Gómez, L., Collins, L., Crous, K. Y., De Kauwe, M. G., dos Santos, B. M., Emmerson, K. M., Facey, S. L., Gherlenda, A. N., Gimeno, T. E., Hasegawa, S., Johnson, S. N.,... Ellsworth, D. S. (2020). The fate of carbon in a mature forest under carbon dioxide enrichment. *Nature*, *580*(7802), 227-231. https://doi.org/10.1038/s41586-020-2128-9
- Jilling, A., Grandy, A. S., Daly, A. B., Hestrin, R., Possinger, A., Abramoff, R., Annis, M., Cates, A. M., Dynarski, K., Georgiou, K., Heckman, K., Keiluweit, M., Lang, A. K., Phillips, R. P., Rocci, K., Shabtai, I. A., Sokol, N. W., & Whalen, E. D. (2025). Evidence for the existence and ecological relevance of fast-cycling mineral-associated organic matter. *Communications Earth & Environment*, 6(1), 690. https://doi.org/10.1038/s43247-025-02681-8
- Klein, T., Bader, M. K. F., Leuzinger, S., Mildner, M., Schleppi, P., Siegwolf, R. T. W., & Körner, C. (2016). Growth and carbon relations of mature *Picea abies* trees under 5 years of free-air CO₂ enrichment. *Journal of Ecology*, 104(6), 1720-1733. https://doi.org/10.1111/1365-2745.12621
 - Kodama, N., Barnard, R. L., Salmon, Y., Weston, C., Ferrio, J. P., Holst, J., Werner, R. A., Saurer, M., Rennenberg, H., Buchmann, N., & Gessler, A. (2008). Temporal dynamics of the carbon isotope composition in a *Pinus sylvestris* stand: from newly assimilated organic carbon to respired carbon dioxide. *Oecologia*, *156*(4), 737-750. https://doi.org/10.1007/s00442-008-1030-1
 - Körner, C. (2015). Paradigm shift in plant growth control. *Current Opinion in Plant Biology*, 25, 107-114. https://doi.org/10.1016/j.pbi.2015.05.003
 - Kuzyakov, Y., & Blagodatskaya, E. (2015). Microbial hotspots and hot moments in soil: Concept & review. *Soil Biology and Biochemistry*, 83, 184-199. https://doi.org/10.1016/j.soilbio.2015.01.025
 - Kuzyakov, Y., & Gavrichkova, O. (2010). REVIEW: Time lag between photosynthesis and carbon dioxide efflux from soil: a review of mechanisms and controls. *Global Change Biology*, 16(12), 3386-3406. https://doi.org/10.1111/j.1365-2486.2010.02179.x
- Lawrence, D. M., Fisher, R. A., Koven, C. D., Oleson, K. W., Swenson, S. C., Bonan, G., Collier, N., Ghimire, B., van Kampenhout, L., Kennedy, D., Kluzek, E., Lawrence, P. J., Li, F., Li, H., Lombardozzi, D., Riley, W. J., Sacks, W. J., Shi, M., Vertenstein, M.,...Zeng, X. (2019). The Community Land Model Version 5: Description of New Features, Benchmarking, and Impact of Forcing Uncertainty. *Journal of Advances in Modeling Earth Systems*, *11*(12), 4245-4287. https://doi.org/10.1029/2018MS001583
- Li, H.-j., Yan, J.-x., Yue, X.-f., & Wang, M.-b. (2008). Significance of soil temperature and moisture for soil respiration in a Chinese mountain area. *Agricultural and Forest Meteorology*, 148(3), 490-503. https://doi.org/10.1016/j.agrformet.2007.10.009
 - Liesche, J., Windt, C., Bohr, T., Schulz, A., & Jensen, K. H. (2015). Slower phloem transport in gymnosperm trees can be attributed to higher sieve element resistance. *Tree Physiology*, 35(4), 376-386. https://doi.org/10.1093/treephys/tpv020
- Liu, Q., Edwards, N. T., Post, W. M., Gu, L., Ledford, J., & Lenhart, S. (2006). Temperature-independent diel variation in soil respiration observed from a temperate deciduous forest. *Global Change Biology*, 12(11), 2136-2145. https://doi.org/10.1111/j.1365-2486.2006.01245.x
 - Lloyd, J., & Taylor, J. A. (1994). On the Temperature Dependence of Soil Respiration. *Functional Ecology*, 8(3), 315-323. https://doi.org/10.2307/2389824

- Martin, J. G., Phillips, C. L., Schmidt, A., Irvine, J., & Law, B. E. (2012). High-frequency analysis of the complex linkage between soil CO₂ fluxes, photosynthesis and environmental variables. *Tree Physiology*, 32(1), 49-64. https://doi.org/10.1093/treephys/tpr134
 - McClain, A. M., & Sharkey, T. D. (2019). Triose phosphate utilization and beyond: from photosynthesis to end product synthesis. *Journal of Experimental Botany*, 70(6), 1755-1766. https://doi.org/10.1093/jxb/erz058
- McElligott, K. M., Seiler, J. R., & Strahm, B. D. (2016). Partitioning soil respiration across four age classes of loblolly pine (*Pinus taeda* L.) on the Virginia Piedmont. *Forest Ecology and Management*, 378, 173-180. https://doi.org/10.1016/j.foreco.2016.07.026
 - Meier, I. C., Finzi, A. C., & Phillips, R. P. (2017). Root exudates increase N availability by stimulating microbial turnover of fast-cycling N pools. *Soil Biology and Biochemistry*, 106, 119-128. https://doi.org/10.1016/j.soilbio.2016.12.004
- Mencuccini, M., & Hölttä, T. (2010). The significance of phloem transport for the speed with which canopy photosynthesis and belowground respiration are linked. *New Phytologist*, 185(1), 189-203. https://doi.org/10.1111/j.1469-8137.2009.03050.x

535

540

- Mitra, B., Miao, G., Minick, K., McNulty, S. G., Sun, G., Gavazzi, M., King, J. S., & Noormets, A. (2019). Disentangling the Effects of Temperature, Moisture, and Substrate Availability on Soil CO₂ Efflux. *Journal of Geophysical Research: Biogeosciences*, 124(7), 2060-2075. https://doi.org/10.1029/2019jg005148
- Mitra, B., Minick, K., Miao, G., Domec, J.-C., Prajapati, P., McNulty, S. G., Sun, G., King, J. S., & Noormets, A. (2020). Spectral evidence for substrate availability rather than environmental control of methane emissions from a coastal forested wetland. *Agricultural and Forest Meteorology*, 291. https://doi.org/10.1016/j.agrformet.2020.108062
- Moyano, F. E., Kutsch, W. L., & Rebmann, C. (2008). Soil respiration fluxes in relation to photosynthetic activity in broadleaf and needle-leaf forest stands. *Agricultural and Forest Meteorology*, 148(1), 135-143. https://doi.org/10.1016/j.agrformet.2007.09.006
 - Myneni, R., Knyazikhin, Y., & Park, T. (2021). MODIS/Terra+Aqua Leaf Area Index/FPAR 4-Day L4 Global 500m SIN Grid V061 (https://doi.org/10.5067/MODIS/MCD15A3H.061
- Noormets, A. (2024). *AmeriFlux BASE US-CRK Davy Crockett National Forest* (Version 5-5) AmeriFlux AMP. https://doi.org/10.17190/AMF/2204055
 - Noormets, A., Gavazzi, M. J., McNulty, S. G., Domec, J.-C., Sun, G. E., King, J. S., & Chen, J. (2010). Response of carbon fluxes to drought in a coastal plain loblolly pine forest. *Global Change Biology*, 16(1), 272-287. https://doi.org/10.1111/j.1365-2486.2009.01928.x
- O'Sullivan, M., Friedlingstein, P., Sitch, S., Anthoni, P., Arneth, A., Arora, V. K., Bastrikov, V., Delire, C., Goll, D. S., Jain,
 A., Kato, E., Kennedy, D., Knauer, J., Lienert, S., Lombardozzi, D., McGuire, P. C., Melton, J. R., Nabel, J. E. M.
 S., Pongratz, J.,...Zaehle, S. (2022). Process-oriented analysis of dominant sources of uncertainty in the land carbon sink. *Nature Communications*, 13(1), 4781. https://doi.org/10.1038/s41467-022-32416-8
 - Ono, M. (2025). Software from: The Use of Newly Assimilated Photosynthates by Soil Autotrophic and Heterotrophic Respiration on a Diurnal Scale. In https://github.com/moekaono/CRK cont SR
- Ono, M., Noormets, A., & Mitchell, S. (2025). The effect of the frequency of prescribed burning on annual soil carbon balance in a loblolly-shortleaf pine forest in East Texas. Frontiers in Forests and Global Change, 8. https://doi.org/10.3389/ffgc.2025.1602557
 - Pataki, D. E., Ehleringer, J. R., Flanagan, L. B., Yakir, D., Bowling, D. R., Still, C. J., Buchmann, N., Kaplan, J. O., & Berry, J. A. (2003). The application and interpretation of Keeling plots in terrestrial carbon cycle research. *Global Biogeochemical Cycles*, 17(1). https://doi.org/https://doi.org/10.1029/2001GB001850
 - Phillips, R. P., Erlitz, Y., Bier, R., & Bernhardt, E. S. (2008). New approach for capturing soluble root exudates in forest soils. Functional Ecology, 22(6), 990-999. https://doi.org/10.1111/j.1365-2435.2008.01495.x
 - Posit team. (2024). RStudio: Integrated Development Environment for R. In (Version 2023.12.1.402) Posit Software, PBC. http://www.posit.co/
- 560 Prescott, C. E. (2022). Sinks for plant surplus carbon explain several ecological phenomena. *Plant and Soil*. https://doi.org/10.1007/s11104-022-05390-9
 - Prescott, C. E., Grayston, S. J., Helmisaari, H.-S., Kaštovská, E., Körner, C., Lambers, H., Meier, I. C., Millard, P., & Ostonen, I. (2020). Surplus Carbon Drives Allocation and Plant–Soil Interactions. *Trends in Ecology & Evolution*, 35(12), 1110-1118. https://doi.org/10.1016/j.tree.2020.08.007

- R Core Team. (2024). R: A Language and Environment for Statistical Computing. In R Foundation for Statistical Computing. https://www.R-project.org/
- Reichstein, M., Falge, E., Baldocchi, D., Papale, D., Aubinet, M., Berbigier, P., Bernhofer, C., Buchmann, N., Gilmanov, T., Granier, A., Grünwald, T., Havránková, K., Ilvesniemi, H., Janous, D., Knohl, A., Laurila, T., Lohila, A., Loustau, D., Matteucci, G.,...Valentini, R. (2005). On the separation of net ecosystem exchange into assimilation and ecosystem respiration: review and improved algorithm. *Global Change Biology*, 11(9), 1424-1439. https://doi.org/10.1111/j.1365-2486.2005.001002.x
 - Roesch, A., & Schmidbauer, H. (2018). *WaveletComp: Computational Wavelet Analysis*. In (Version 1.1) https://CRAN.R-project.org/package=WaveletComp
 - Savage, K., Davidson, E. A., & Tang, J. (2013). Diel patterns of autotrophic and heterotrophic respiration among phenological stages. *Global Change Biology*, 19(4), 1151-1159. https://doi.org/10.1111/gcb.12108

- Sevanto, S., & Dickman, L. T. (2015). Where does the carbon go?—Plant carbon allocation under climate change. *Tree Physiology*, *35*(6), 581-584. https://doi.org/10.1093/treephys/tpv059
- Tang, J., Baldocchi, D. D., & Xu, L. (2005). Tree photosynthesis modulates soil respiration on a diurnal time scale. *Global Change Biology*, 11(8), 1298-1304. https://doi.org/10.1111/j.1365-2486.2005.00978.x
- Thompson, M. V., & Holbrook, N. M. (2004). Scaling phloem transport: information transmission. *Plant, Cell & Environment*, 27(4), 509-519. https://doi.org/10.1111/j.1365-3040.2003.01148.x
 - van't Hoff, J. H. (1898). Lectures on theoretical and physical chemistry Part I. chemical dynamics (R. A. Lehfeldt, Trans.). E. Arnold.
- Vargas, R., Baldocchi, D. D., Bahn, M., Hanson, P. J., Hosman, K. P., Kulmala, L., Pumpanen, J., & Yang, B. (2011). On the multi-temporal correlation between photosynthesis and soil CO₂ efflux: reconciling lags and observations. *New Phytol*, 191(4), 1006-1017. https://doi.org/10.1111/j.1469-8137.2011.03771.x
 - Vargas, R., Detto, M., Baldocchi, D. D., & Allen, M. F. (2010). Multiscale analysis of temporal variability of soil CO₂ production as influenced by weather and vegetation. *Global Change Biology*, 16(5), 1589-1605. https://doi.org/10.1111/j.1365-2486.2009.02111.x
- Wingate, L., Ogée, J., Burlett, R., Bosc, A., Devaux, M., Grace, J., Loustau, D., & Gessler, A. (2010). Photosynthetic carbon isotope discrimination and its relationship to the carbon isotope signals of stem, soil and ecosystem respiration. New Phytologist, 188(2), 576-589. https://doi.org/10.1111/j.1469-8137.2010.03384.x
 - Wutzler, T., Reichstein, M., Moffat, A. M., & Migliavacca, M. (2022). REddyProc: Post Processing of (Half-)Hourly Eddy-Covariance Measurements. R package version 1.3.2. In https://CRAN.R-project.org/package=REddyProc
- Yang, Z. J., Lin, T. C., Wang, L. X., Chen, S. D., Liu, X. F., Xiong, D. C., Xu, C., Arthur, M., McCulley, R., Shi, S. H., & Yang, Y. S. (2022). Recent Photosynthates Are the Primary Carbon Source for Soil Microbial Respiration in Subtropical Forests. *Geophysical Research Letters*, 49(22), Article e2022GL101147. https://doi.org/10.1029/2022gl101147
 - Yin, H., Wheeler, E., & Phillips, R. P. (2014). Root-induced changes in nutrient cycling in forests depend on exudation rates. *Soil Biology and Biochemistry*, 78, 213-221. https://doi.org/10.1016/j.soilbio.2014.07.022
 - Zweifel, R., Sterck, F., Braun, S., Buchmann, N., Eugster, W., Gessler, A., Häni, M., Peters, R. L., Walthert, L., Wilhelm, M., Ziemińska, K., & Etzold, S. (2021). Why trees grow at night. *New Phytologist*, 231(6), 2174-2185. https://doi.org/10.1111/nph.17552